European Conferences on Biomedical Optics 2025 © Optica Publishing Group-SPIE 2025

Exploiting Spectral Signatures for Retinal Health Assessment: A Phasor Analysis Approach

Armin Eskandarinasab,[1,*] Laura Rey-Barroso,[1] Francisco J. Burgos-Fernández, [1] Meritxell Vilaseca[1]

[1] *Center for Sensors, Instruments and Systems Development, Universitat Politècnica de Catalunya, Rambla Sant Nebridi 10, Terrassa, 08222, Spain*

[*] *armin.eskandarinasab@upc.edu*

Abstract: This study applies phasor analysis to multispectral retinal images for automated classification of healthy and diseased cases, achieving high accuracy with a ν-SVM classifier and first harmonic for the entire retina and macular region.

1. Introduction

Retinography provides a detailed, non-invasive view of the eye fundus, allowing ophthalmologists to examine key structures such as blood vessels, the optic disc, and the macula. With advancements in machine and deep learning, fundus imaging has become an essential tool for detecting abnormalities, diagnosing retinal diseases, and guiding personalized treatment plans. For instance, a study [1] introduced a novel convolutional neural network model for predicting diabetic retinopathy from fundus images, outperforming existing methods. Ordinary fundus cameras typically use color sensors with three broad RGB bands to capture image data. In contrast, multispectral imaging provides a more advanced approach by capturing information across a wider range of wavelengths, including those beyond the visible (VIS) spectrum. These additional wavelengths, particularly in the near-infrared (NIR) range, can penetrate deeper layers of the fundus, potentially revealing subtle changes and critical details.

Multispectral data exhibits moderate inter-band correlation, a characteristic that, while providing valuable spectral information, also necessitates careful handling of potential redundancy. Phasor analysis [2] offers a promising approach to address this challenge by mapping high-dimensional multispectral data onto a two-dimensional plane while preserving essential information. This dimensionality reduction technique has proven effective in various fields dealing with complex datasets. For instance, Parra et al. [3] successfully employed phasor analysis to interpret high-dimensional embryo data from multispectral records.

This study investigates the application of phasor analysis to multispectral retinal images. By combining this compact representation with machine learning algorithms, a screening tool has been developed to classify retinas as healthy or diseased. The underlying hypothesis is that reducing redundant data through phasor analysis will enhance the accuracy and reliability of retinal disease classification.

2. Materials

2.1. Spectral Retinograph

Multispectral images were acquired using a custom-built, area-scanning multispectral fundus camera, detailed in [4]. The device features an optical system with an array of LEDs, each emitting light at a specific peak wavelength, and two cameras: a high-resolution CMOS sensor (2048×2048 pixels, pixel size 6.5 μm, and 16-bit depth) that captures 12 spectral images ranging from 416 to 955 nm, and a lower-resolution InGaAs camera (640×512 pixels, pixel size 20 μm, and 14-bit depth) that captures images in three bands from 1025 to 1213 nm. After post-processing and cropping, images with 1757×1757 pixels and 386 x 386 pixels remain for the CMOS and InGaAs cameras, respectively. In this study, the three NIR images from the InGaAs camera were excluded due to its lower resolution and higher noise levels compared to the CMOS sensor.

2.2. Data Collection

A dataset of multispectral images from 102 retinas (50 diseased and 52 healthy cases which are 1224 images in total) was used. The diseased retinas included conditions such as Age-related Macular Degeneration (AMD), epiretinal membrane, and retinal detachment, among others. Images were collected at the Instituto de Microcirugia Ocular (IMO - Miranza Group, Barcelona, Spain) and the Vision University Center (CUV) of the Universitat Politècnica de Catalunya (Terrassa, Spain) [5].

2.3. *Phasor Analysis & Machine Learning*

Phasor analysis was computed for each pixel in the spectral cube of a sample (x, y, λ). This spectrum is represented as a complex number with real and imaginary components $(g_{x,y} + is_{x,y})$ and processed using a discrete Fourier transform [2]. Real and imaginary parts are defined as follows:

$$g_{x,y}(k) = \frac{\sum_{\lambda_0}^{\lambda_n} I_{x,y}(\lambda) * \cos(\frac{2\pi k\lambda}{2}) * \Delta\lambda}{\sum_{\lambda_0}^{\lambda_n} I_{x,y}(\lambda) * \Delta\lambda}, s_{x,y}(k) = \frac{\sum_{\lambda_0}^{\lambda_n} I_{x,y}(\lambda) * \sin(\frac{2\pi k\lambda}{2}) * \Delta\lambda}{\sum_{\lambda_0}^{\lambda_n} I_{x,y}(\lambda) * \Delta\lambda}$$

where λ_0 and λ_n represent the wavelengths of the first and last bands of the multispectral image, respectively. n denotes the number of spectral channels in the spectral cube, $\Delta\lambda$ represents the bandwidth of a single channel, and k refers to the harmonic number. To investigate the influence of harmonics, the first and second harmonics were compared in this study. Once each fundus image is encoded into $g_{x,y}$ and $s_{x,y}$ components, an average value was calculated for each sample, resulting in a single vector (g_{avg}, s_{avg}) per image, referred to as the averaged representation (Fig. 1).

Furthermore, two processing approaches were employed: one using the entire fundus image and the other focusing solely on the macular region. The dataset was processed to exclude images of diseases outside the macular region. Nine diseased retinas were excluded because the pathology did not affect the macula, and to maintain a balanced dataset, 11 healthy retinas were also removed. This resulted in a final dataset of 41 diseased, and 41 healthy cases. The analysis focused on the macular region along with a small surrounding area. While the exact size varied slightly across images, the region of interest averaged approximately 400×400 pixels.

The averaged phasor representation served as input for four different classification algorithms to distinguish between healthy and diseased retinas: Nearest Centroid (NC), Gaussian Naive Bayes (GNB), Support Vector Machine (SVM), and ν-SVM [6].

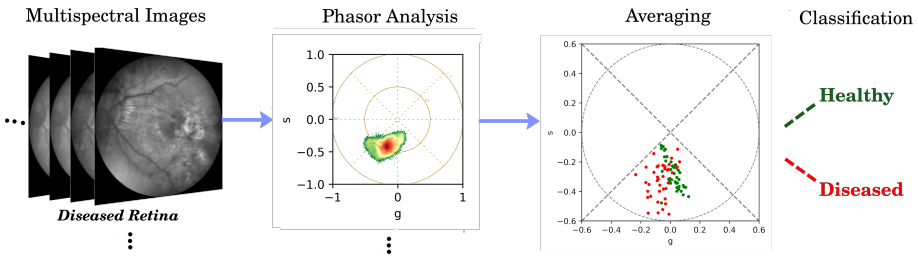

Fig. 1. From left to right: multispectral fundus images are mapped into the phasor plots for a particular harmonic. The plots show all pixels of a spectral cube, i.e., a sample. These are then condensed into a single average phasor value, which serves as the input for classification algorithms, ultimately distinguishing between healthy and diseased retinas.

3. Results

A graphical comparison between g_{avg} and s_{avg} for the 102 retinas analyzed is depicted in Fig. 2. Only averaged data for the entire fundus and the macular region are shown for both the first and second harmonic components. Table 1 shows the performance metrics in classifying between healthy and diseased retinas evaluated using several algorithms. Our findings indicate that the combination of phasor analysis with machine learning algorithms,

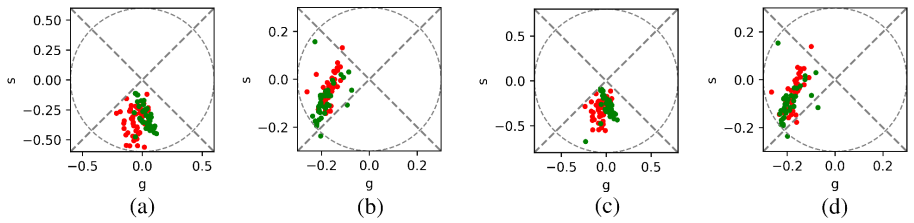

Fig. 2. Average representations for a) entire retina on 1st harmonic, b) entire retina on 2nd harmonic, c) macular region on 1st harmonic, d) macular region on 2nd harmonic

specifically ν-SVM, can effectively distinguish between healthy and diseased retinas. The best results are achieved using the first harmonic, regardless of whether the analysis covers the entire retina or focuses only on the macula.

Table 1. Performance of the classification algorithms using the entire retina with 1st and 2nd harmonics. Overall Accuracy (OA), Balanced Accuracy (BA), Specificity, Sensitivity, and F1-score. The numbers in bold are the best results.

Retina Section	Method	Harmonic	OA	BA	F1-Score	Specificity	Sensitivity
Entire	NC	1st	0.77	0.76	0.73	**0.86**	0.67
		2nd	0.66	0.66	0.66	0.62	0.70
	GNB	1st	0.74	0.75	0.74	0.73	0.76
		2nd	0.64	0.65	0.67	0.56	0.74
	SVM	1st	0.77	0.77	0.74	0.84	0.70
		2nd	0.67	0.67	0.69	0.56	0.78
	ν-SVM	1st	**0.78**	**0.78**	**0.77**	0.78	0.78
		2nd	0.69	0.69	0.71	0.58	**0.80**
Macula	NC	1st	0.70	0.71	**0.76**	0.76	0.65
		2nd	0.61	0.62	0.60	0.67	0.57
	GNB	1st	0.70	0.71	0.69	0.75	0.67
		2nd	0.66	0.67	0.66	0.70	0.64
	SVM	1st	0.74	0.75	0.74	0.78	0.71
		2nd	0.59	0.60	0.61	0.57	0.63
	ν-SVM	1st	**0.77**	**0.78**	**0.76**	**0.84**	**0.72**
		2nd	0.66	0.67	0.67	0.67	0.67

4. Conclusion

This study has demonstrated the potential of phasor analysis for classifying healthy and diseased retinas using multispectral retinal images. By reducing the dimensionality of the multispectral data, phasor analysis simplifies the information while retaining crucial diagnostic features.

Future research will explore the incorporation of multiple harmonics to potentially extract even more nuanced spectral information. Additionally, analysis will be tailored to specific image regions affected by disease, such as the optic disc, macula, or vessels. Furthermore, the application of deep learning architectures for classification will be investigated, which may offer improved performance and the ability to automatically learn complex features from the phasor representations. Ultimately, the fusion of multispectral data with other imaging modalities, such as Optical Coherence Tomography (OCT), is also envisioned.

Acknowledgements

Funded by European Union (HORIZON–MSCA–2022–DN, GA nº101119924–BE-LIGHT) and by MCIU /AEI /10.13039/501100011033 and FEDER, EU (Grant PID2023-147541OB-I00).

References

1. V Banupriya and S Anusuya. Improving classification of retinal fundus image using flow dynamics optimized deep learning methods. *arXiv preprint arXiv:2305.00294*, 2023.
2. Leonel Malacrida, Enrico Gratton, and David M Jameson. Model-free methods to study membrane environmental probes: a comparison of the spectral phasor and generalized polarization approaches. *Methods and applications in fluorescence*, 3(4):047001, 2015.
3. Albert Parra, Denitza Denkova, Xavier P Burgos-Artizzu, Ester Aroca, Marc Casals, Amélie Godeau, Miguel Ares, Anna Ferrer-Vaquer, Ot Massafret, Irene Oliver-Vila, et al. Metaphor: Metabolic evaluation through phasor-based hyperspectral imaging and organelle recognition for mouse blastocysts and oocytes. *Proceedings of the National Academy of Sciences*, 121(28):e2315043121, 2024.
4. Tommaso Alterini, Fernando Díaz-Doutón, Francisco J Burgos-Fernández, Laura González, Carlos Mateo, and Meritxell Vilaseca. Fast visible and extended near-infrared multispectral fundus camera. *Journal of biomedical optics*, 24(9):096007–096007, 2019.
5. Francisco J Burgos-Fernández, Tommaso Alterini, Fernando Díaz-Doutón, Laura González, Carlos Mateo, Clara Mestre, Jaume Pujol, and Meritxell Vilaseca. Reflectance evaluation of eye fundus structures with a visible and near-infrared multispectral camera. *Biomedical optics express*, 13(6):3504–3519, 2022.
6. Bernhard Schölkopf, Alex J Smola, Robert C Williamson, and Peter L Bartlett. New support vector algorithms. *Neural computation*, 12(5):1207–1245, 2000.